Journal of the European Ceramic Society 22 (2002) 2689–2696

www.elsevier.com/locate/jeurceramsoc

Tailoring the mechanical properties of silicon carbide ceramics by modification of the intergranular phase chemistry and microstructure

You Zhou*, Kiyoshi Hirao, Yukihiko Yamauchi, Shuzo Kanzaki

Synergy Materials Research Center, National Institute of Advanced Industrial Science and Technology (AIST), 2268-1 Shimo-Shidami, Moriyama-ku, Nagoya 463-8687, Japan

Received 7 November 2001; received in revised form 21 February 2002; accepted 29 March 2002

Abstract

Liquid-phase-sintered SiC has attracted increasing interest for its ability to form an in-situ toughened material and its potentially superior mechanical properties relative to the solid-state-sintered SiC. In the present work, a submicron-size β-SiC powder was densified with additives of various combinations of rare-earth oxides (RE_2O_3; RE = La, Nd, Y and Yb) and alumina by hot-pressing, and the hot-pressed materials were further annealed at higher temperatures. The phase compositions, microstructures and mechanical properties of the hot-pressed and the annealed materials were characterized. It was found that the mechanical properties were strongly influenced by the type of the sintering additives. The additives also affected the microstructural development during annealing. While the fracture toughness of all the annealed materials continuously increased with increasing annealing temperatures, however, the flexural strength either increased or decreased with annealing temperatures, depending on the kinds of the RE_2O_3 additives. By using appropriate rare-earth oxides, e.g. La_2O_3 or Nd_2O_3, fracture toughness and flexural strength synergetically improved after an annealing treatment.

Keywords: Annealing; Grain boundary phase; Mechanical properties; Microstructure-final; SiC

1. Introduction

The densification of silicon carbide powders always needs the aid of sintering additives due to the high covalency of Si–C bond and the low self-diffusion coefficient.[1] Depending on the kinds of doped sintering aids, SiC may be densified by either a solid-state or liquid-phase sintering mechanism. Nowadays, solid-state-sintering of SiC with boron- and carbon-containing substances as sintering additives has become a key technology of manufacturing SiC mechanical components in industry, however, some inherent problems associated with this method such as the low flexural strength and low fracture toughness of the solid-state-sintered SiC make it unsuitable for use in many applications. Recent studies reveal that to sinter SiC ceramics by another method, i.e. liquid-phase-sintering, may provide a way to improve the mechanical properties of SiC.[2–11]

In liquid-phase-sintered SiC (LPS–SiC), sintering additives react with the surface oxide on SiC powder particles to provide a mass transport medium during densification, and they finally result in the formation of secondary phases at grain boundaries. For a liquid-phase-sintered material, the intergranular phase could strongly affect its properties. For instance, silicon nitride is a typical liquid-phase-sintered ceramic material, and studies on the intergranular phase itself and its influence on the mechanical properties of Si_3N_4 have been extensively conducted. Becher et al.[12,13] found that the chemical composition of the grain boundary amorphous phase could significantly influence the interfacial debonding behavior in silicon nitrides. Kleebe et al.[14] also showed that the secondary-phase chemistry could play a key role in toughening Si_3N_4 ceramics, due to its influences on the Si_3N_4-grain morphology formation, secondary-phase crystallization and residue stress distribution at the grain boundaries.

However, unlike Si_3N_4 ceramics, the influence of intergranular phase on SiC ceramics has not been systematically examined. And, earlier studies on LPS–SiC have predominantly employed mixtures of Al_2O_3 and

* Corresponding author. Tel.: +81-52-739-0133; fax: +81-52-739-0136.

E-mail address: you.zhou@aist.go.jp (Y. Zhou).

0955-2219/02/$ - see front matter
PII: S0955-2219(02)00134-6

Y_2O_3 as sintering additives. Work on sintering of SiC with other additives is very limited. Recently,[15] we found that a variety of rare-earth oxides (RE_2O_3) were as effective as Y_2O_3 in aiding densification of SiC, and the SiC ceramics containing different RE_2O_3 additives had different mechanical properties although their microstructures were almost equally fine and equiaxed. The changes of the mechanical properties revealed that a decrease in the cationic radius of the RE_2O_3 was accompanied by an increase in Young's modulus, hardness and flexural strength and a decrease in fracture toughness of the SiC ceramics. That trend was attributed to the difference in the chemistry of the intergranular phases. As a continuation of that work, the present study used four RE_2O_3 (RE = La, Nd, Y and Yb) in combination with Al_2O_3 as sintering additives for a submicron-size β-SiC. The powder mixtures were densified by hot-pressing, and then annealed at higher temperatures in order to form a so-called in-situ-toughened material consisting of large elongated grains.[2] The purpose was to investigate how the microstructural evolution during heat treatment was affected by the sintering additives and hence, the intergranular phase chemistry, and how the mechanical properties of SiC ceramics could be tailored by modification of the intergranular phase chemistry and microstructure.

2. Experimental procedure

The starting powder was high purity β-SiC (UF, Ibiden Co., Gifu, Japan) with an average particle size of 0.30 μm and specific surface area of 20.0 m^2/g. The main impurity was 0.25 wt.% oxygen. The additives were Al_2O_3 (AKP50, Sumitomo Chemicals, Tokyo, Japan) and four rare-earth oxides: La_2O_3, Nd_2O_3, Y_2O_3 and Yb_2O_3 (99.9% pure, Nippon Yttrium Co., Tokyo, Japan). Four batches of powders (see Table 1) were prepared, each containing 95 vol.% SiC and 5 vol.% ($Al_2O_3 + RE_2O_3$) (RE = La, Nd, Y and Yb). The additive composition (molar ratio of Al_2O_3:RE_2O_3) of each batch was selected at the lowest eutectic point in the Al_2O_3–RE_2O_3 phase diagram, so that the powers could be densified at relatively low temperatures with little grain coarsening. The lowest eutectic point is around 1780 °C for Al_2O_3–La_2O_3 system,[16] 1720 °C for Al_2O_3–Nd_2O_3 system,[17] 1760 °C for Al_2O_3–Y_2O_3 system,[18] and 1750 °C for Al_2O_3–Yb_2O_3 system.[19] The specimen designations are given in Table 1.

The mixtures of SiC and additives were blended in methanol in an SiC planetary mill, then dried with a rotary evaporator, crushed, and screened through a 60-mesh sieve. The mixed powder was hot-pressed at 1800 °C for 1 h under a pressure of 40 MPa in argon atmosphere. The final hot-pressed block size was 42×47×5 mm. For each composition, more than six blocks were prepared. Some of the hot-pressed blocks were given a further annealing treatment at 1850 or 1950 °C for 3 h under an atmosphere of argon in a graphite resistance furnace.

Bulk densities were measured by the Archimedes method. The hot-pressed and the annealed specimens were cut, polished, and etched by a plasma of CF_4 containing 10% O_2 in a commercial plasma etching apparatus (model PR31Z, Yamato Scientific, Tokyo, Japan). The microstructures of the etched surfaces were observed by a scanning electron microscope (SEM; model JSM-6340F, Jeol, Tokyo, Japan) equipped with a field emission gun. Quantitative analyses on digitized SEM photographs were carried out using an image analysis software (Scion Image, Scion Corporation, Frederick, USA). For each specimen at least 2000 grains were measured. The area (A_{grain}), shortest and longest diagonals of each grain in a sectioned plane were automatically determined by the software. The equivalent grain diameter (D) of each grain was calculated by the equation $D = 2\left(A_{grain}/\pi\right)^{1/2}$,[20] and it was defined as the grain size in this study. The grain-size distribution was evaluated by plotting the fractional cumulative area of the grains versus the corresponding calculated equivalent grain diameters. The mean grain diameter was considered to be the value for one-half the cumulative area.[21] Considering an elongated grain morphology, the width (W) and length (L) of each grain were obtained from the shortest and the longest diagonals in a two-dimensional image, respectively. The mean value of the 10% highest apparent aspect ratios (L/W) was considered to be the mean of the actual aspect ratios (R_{95}).[21–23]

X-ray diffraction analysis (XRD; RINT2500, Rigaku, Tokyo, Japan) with CuK_α radiation of 40 kV/100 mA was performed on ground powders of the hot-pressed and the annealed materials for phase identification.

Table 1
Compositions and specimen designations of various mixtures

Specimen designation	RE_2O_3	Ionic radius of RE^{3+}(nm)	Composition (vol.%)		
			β-SiC	Al_2O_3	RE_2O_3
AlLa5	La_2O_3	0.1061	95	3.19	1.81
AlNd5	Nd_2O_3	0.0995	95	3.25	1.75
AlY5	Y_2O_3	0.0892	95	3.28	1.72
AlYb5	Yb_2O_3	0.0858	95	3.49	1.51

Test beams with dimensions of 4×3×42 mm were sectioned and ground with a 400-grit diamond grinding wheel. The beams were tested in a four-point bending jig with an outer span of 30 mm, an inner span of 10 mm, and at a crosshead speed of 0.5 mm/min. The tensile surfaces of the specimens were polished to a 1/2 μm diamond finish, and the edges were chamfered to reduce edge flaws. Fracture toughness and hardness were measured by the indentation fracture (IF) method and calculated using the equations proposed by Anstis et al.[24] Ten indentations were made by a Vickers indenter at 98 N load on the polished surface of each sample. Young's modulus was measured by the pulse-echo method. The indented surfaces were also plasma-etched and observed by use of SEM in order to examine the crack/microstructure interactions.

3. Results

3.1. The hot-pressed materials

Doped with 5 vol.% $Al_2O_3 + RE_2O_3$ (RE = La, Nd, Y and Yb) and hot-pressed at 1800 °C for 1 h, all specimens were densified to near theoretical densities, and they all exhibited similarly fine and equiaxed microstructures (Fig. 1) consisting of β-SiC grains and partially crystallized intergranular phases. However, their mechanical properties were quite different. There was a correlation between the mechanical properties and the cationic radii of the doped RE_2O_3, i.e. the flexural strength decreased with the increase in the cationic radius of RE_2O_3, whereas the fracture toughness increased with the increase in the cation size. The measured strength and toughness of specimens AlLa5, AlNd5, AlY5 and AlYb5 were 504, 550, 587 and 652 MPa, and 4.2, 3.9, 3.7 and 3.4 $MPa{\cdot}m^{1/2}$, respectively. Those changes in the mechanical properties were attributed to the varying grain boundary strength resulting from the different intergranular phase chemistry. The related discussion in greater detail can be found in Ref. 15.

3.2. Effect of annealing on microstructural development

The four hot-pressed SiC ceramics were annealed at 1850 or 1950 °C for 3 h. Fig. 2 shows the microstructures of the materials annealed at 1850 °C. Compared with the hot-pressed materials (Fig. 2 versus Fig. 1), grain sizes have become larger in all the annealed materials. However, the extent of grain coarsening and the resulted grain morphologies between the materials were different. In the annealed AlLa5 and AlNd5, there were a few large elongated grains. In the annealed AlYb5, almost all grains were large and elongated. In contrast, almost

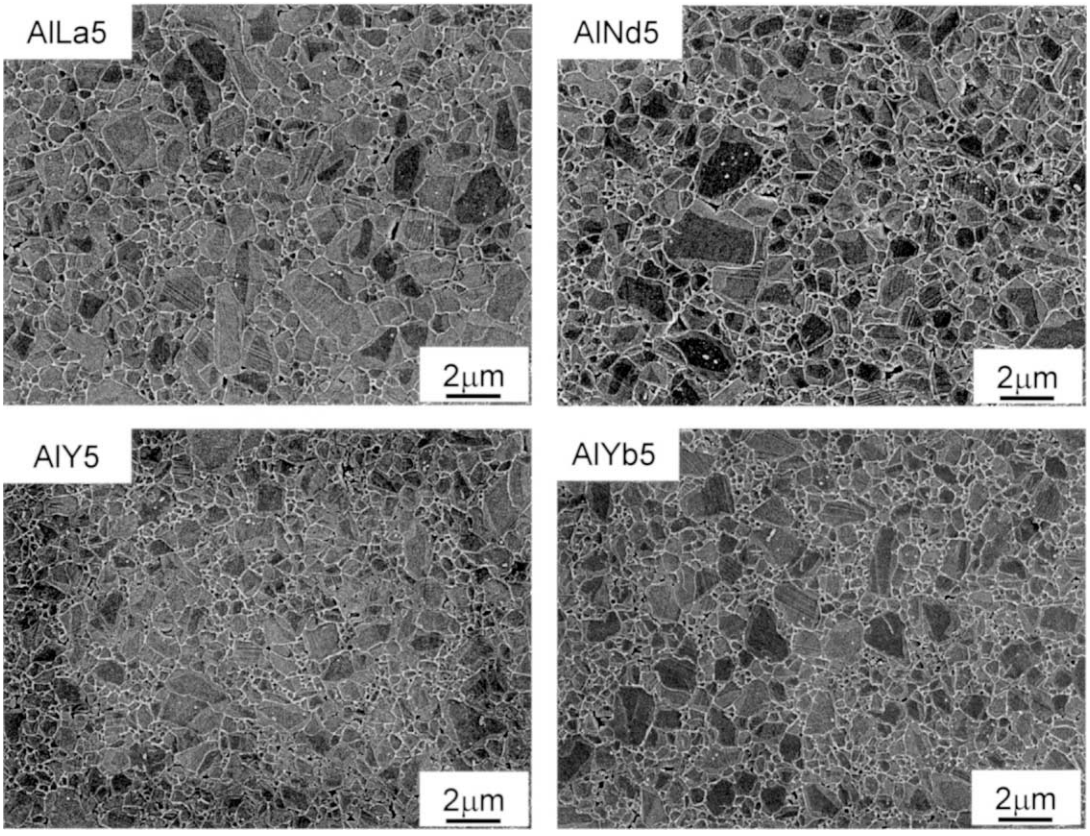

Fig. 1. SEM micrographs of the polished and plasma-etched surfaces of the four hot-pressed SiC ceramics.

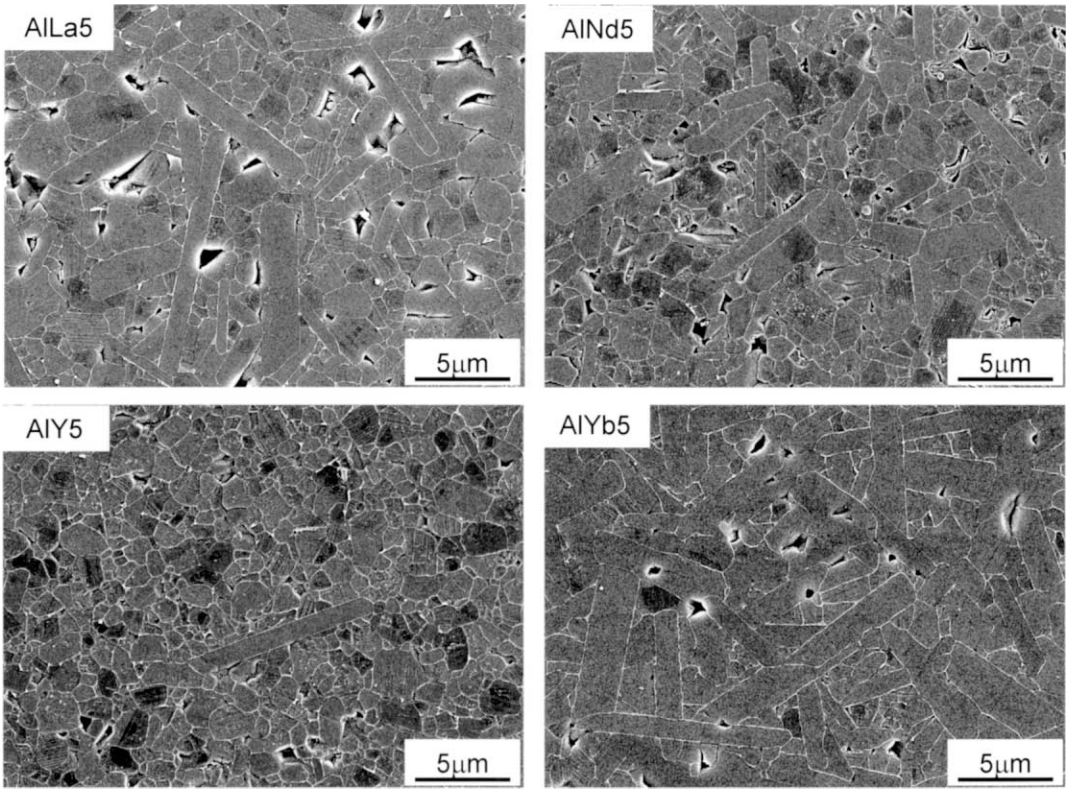

Fig. 2. SEM micrographs of the polished and plasma-etched surfaces of the four SiC ceramics after being annealed at 1850 °C.

all grains in the annealed AlY5 remained to be equiaxed except that very few elongated grains occasionally appeared in the microstructure.

Fig. 3 shows the microstructures of the materials annealed at 1950 °C. In the 1950 °C-annealed AlLa5 and AlNd5, nearly all grains have grown to be elongated. In the 1950 °C-annealed AlYb5, the elongated grains were thicker than those in the 1850 °C-annealed AlYb5. The 1950 °C-annealed AlY5 consisting of large plate-like grains, turned to have the coarsest microstructure among the four 1950 °C-annealed materials, although the microstructure of the 1850 °C-annealed AlY5 was the finest among the four 1850 °C-annealed materials.

3.3. Effect of annealing on mechanical properties

Figs. 4 and 5 show the fracture toughness and flexural strength of the hot-pressed, 1850°C- and 1950 °C-annealed SiC ceramics, respectively. For all the materials, an annealing treatment always had a positive impact on the fracture toughness, and, the higher the annealing temperature, the greater gain in the toughness. In contrast, the influence of annealing on the flexural strength might be positive or negative, depending on material and annealing temperature. After being annealed at 1850 °C, the flexural strength of all materials improved. With the annealing temperature increasing to 1950 °C, however, while the strength of the annealed AlLa5 and AlNd5 kept on improving, the annealed AlY5 and AlYb5 suffered a serious strength-degradation.

Among all the materials, the 1950 °C-annealed AlLa5 and AlNd5 had the best mechanical properties. The flexural strength and fracture toughness of the 1950 °C-annealed AlLa5 were 661 MPa and 5.5 $MPa{\cdot}m^{1/2}$, respectively; and the values for the 1950 °C-annealed AlNd5 attained 620 MPa and 5.5 $MPa{\cdot}m^{1/2}$, respectively.

4. Discussion

For the SiC ceramics obtained by low temperature hot-pressing, where grain growth were suppressed, the intergranular phase chemistry could influence the mechanical properties by varying the grain boundary strength.[15] For the SiC resulting from annealing the hot-pressed materials at higher temperatures, where grain coarsening occurred, the intergranular phase should have exerted an influence on the growth of the SiC grains. That means, an annealing treatment would enable the intergranular phase chemistry to tailor the mechanical properties not only by directly modulating the grain boundary strength, but also through its influences on the development of the final microstructures. This has been verified by the previously mentioned experimental results, and it will be more clearly shown in the following discussion.

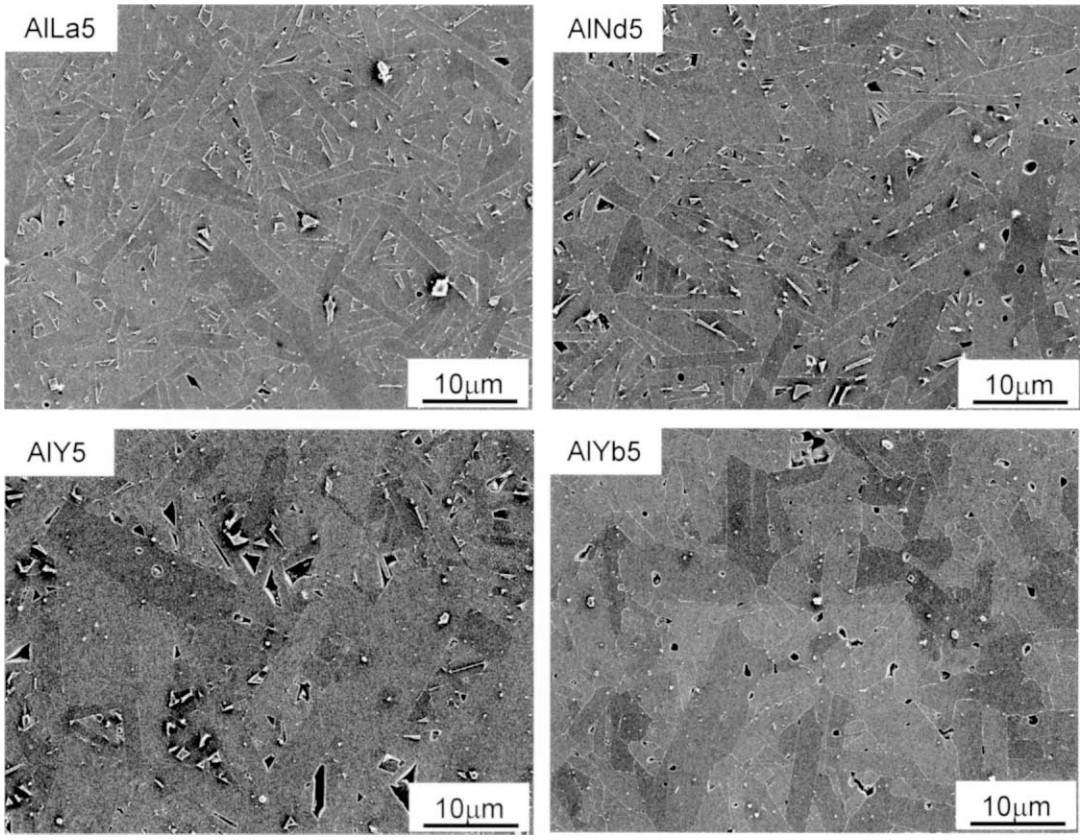

Fig. 3. SEM micrographs of the polished and plasma-etched surfaces of the four SiC ceramics after being annealed at 1950 °C.

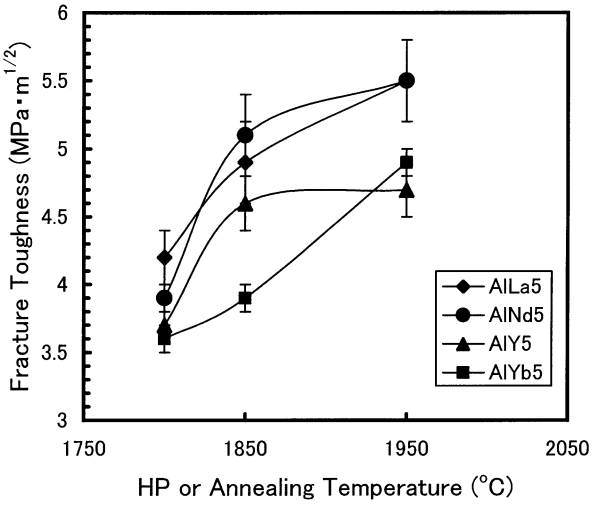

Fig. 4. Fracture toughness of the hot-pressed, 1850 and 1950 °C-annealed SiC ceramics.

The microstructures of the SiC doped with various additives developed during annealing have been shown in Figs. 2 and 3. An image analysis on those micrographs will yield additional information on the influences of the additives on the microstructural development. Fig. 6 shows the mean grain sizes (i.e. mean equivalent grain diameters) of the hot-pressed and the annealed materials. Fig. 7 shows the mean aspect ratios (R_{95}) of those materials. The aspect ratio of the hot-pressed SiC is considered to be 1 for equiaxed microstructure.[10]

Annealed at 1850 °C, the grain growth in AlY5 was the smallest, and that in AlYb5 was the largest and most anisotropic among the four materials. The grain coarsening of all materials should have contributed to their increased fracture toughness.[25,26] The toughening mechanism is thought to be the enhanced crack deflection and crack bridging by the large and elongated grains, as evidenced by the crack propagation features shown in Fig. 8. A very interesting finding is that both the flexural strength and fracture toughness of all materials improved after 1850 °C-annealing, in contrast to the well-known "trade-off" in improving toughness and strength of SiC ceramics, i.e. a coarse microstructure is beneficial for toughness but detrimental for strength, and vice versa.[5,6,23,27] The improved flexural strength might be attributed to the interlocking force between the elongated grains and the effect of the increased toughness, under the condition that the grain sizes were not too large. In the four 1850 °C-annealed materials, the biggest mean equivalent grain diameter (of the annealed AlYb5) was just 2.4 μm (Fig. 6).

With the annealing temperature increasing to 1950 °C, AlY5 underwent the fastest grain growth and formed the coarsest microstructure among the four 1950 °C-annealed materials. AlYb5 also underwent enormous

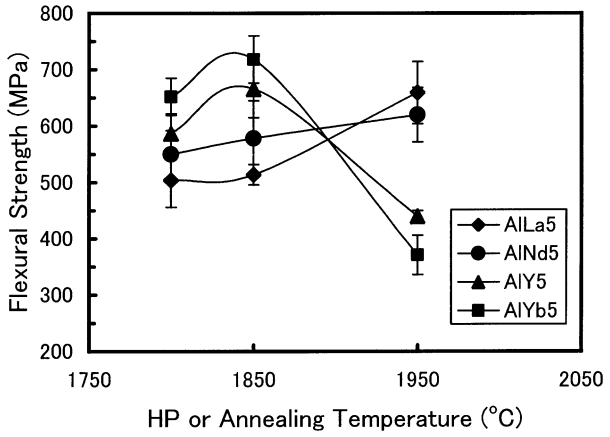

Fig. 5. Flexural strength of the hot-pressed, 1850 and 1950 °C-annealed SiC ceramics.

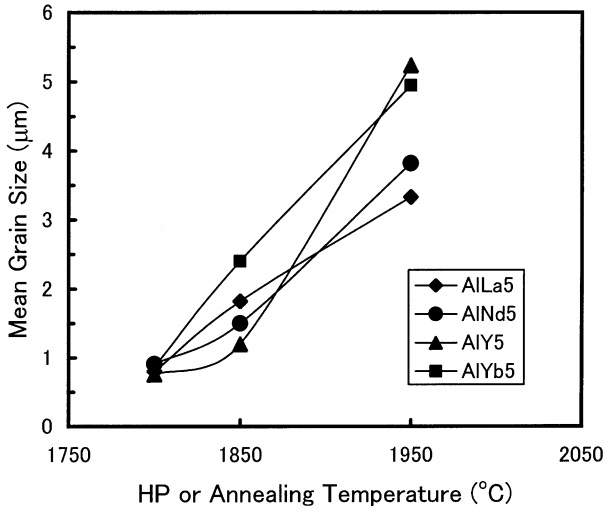

Fig. 6. Mean grain sizes (i.e. mean equivalent grain diameters) of the hot-pressed, 1850 and 1950 °C-annealed SiC ceramics.

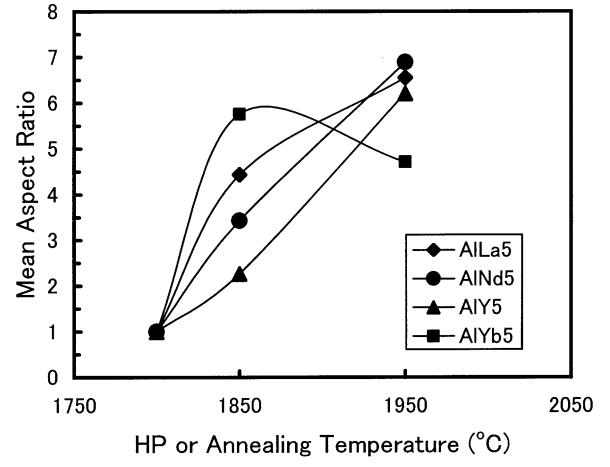

Fig. 7. Mean aspect ratios (R_{95}) of the hot-pressed, 1850 and 1950 °C-annealed SiC ceramics.

grain growth, but the growth was less anisotropic than that during 1850 °C-annealing; thus the 1950 °C-annealed AlYb5 had a decreased mean aspect ratio. The mean equivalent grain diameters of the 1950 °C-annealed AlLa5 and AlNd5 were the smallest, however their aspect ratios were the largest (Figs. 6 and 7), indicating that the grain growth in these two materials was very anisotropic. Thus, the four 1950 °C-annealed materials could be divided into two groups, with one including the annealed AlLa5 and AlNd5, and the other including the annealed AlY5 and AlYb5. The former had smaller grain sizes and larger aspect ratios than the latter. The relatively small grain sizes and large aspect ratios of the 1950 °C-annealed AlLa5 and AlNd5 might account for the further improved flexural strength and fracture toughness over their 1850 °C-annealed counterparts. In the case of the 1950 °C-annealed AlY5 and AlYb5, the coarser microstructures contributed to the higher fracture toughness than their 1850 °C-annealed counterparts; however, they also resulted in the serious decreases in their flexural strength. It implies that there may exist critical parameters for the ranges of grain size and aspect ratio for a ceramic material, within which grain coarsening can lead to simultaneous improvement of toughness and strength; however, beyond the ranges grain coarsening will deteriorate the strength, i.e. the law of "trade-off" takes effect at that time.

It is clearly shown earlier that structural parameters such as grain size and aspect ratio could affect the mechanical properties of SiC ceramics, however, the microstructure was not the only influencing factor. The mechanical properties were also influenced by the intergranular phase composition. For instance, after being annealed at 1850 °C, the annealed AlYb5 was composed of large and elongated grains, while the annealed AlNd5 had smaller grain size and aspect ratio (Figs. 6 and 7); however, the latter had higher fracture toughness than the former (5.1 versus 3.9 $MPa{\cdot}m^{1/2}$, Fig. 4). To understand this, the crack propagation behaviors in the two materials were examined. As shown in Fig. 8, although not being quantified, more frequently occurred crack deflection and crack bridging were observed in the annealed AlNd5 than in the annealed AlYb5. More crack deflection and crack bridging could result in a stronger toughening effect, which was thought to have contributed to the higher fracture toughness of the annealed AlNd5 than that of the annealed AlYb5. The difference in the crack propagation behaviors might be owing to the difference in the grain boundary strength of the annealed materials that had different intergranular phase chemistry, similar to the case of the hot-pressed materials reported in Ref. 15.

XRD analyses revealed that β- to α-SiC phase transformation occurred during annealing of all materials. The elongated grains appeared in the microstructures of the sectioned planes (Figs. 2 and 3) could be regarded as

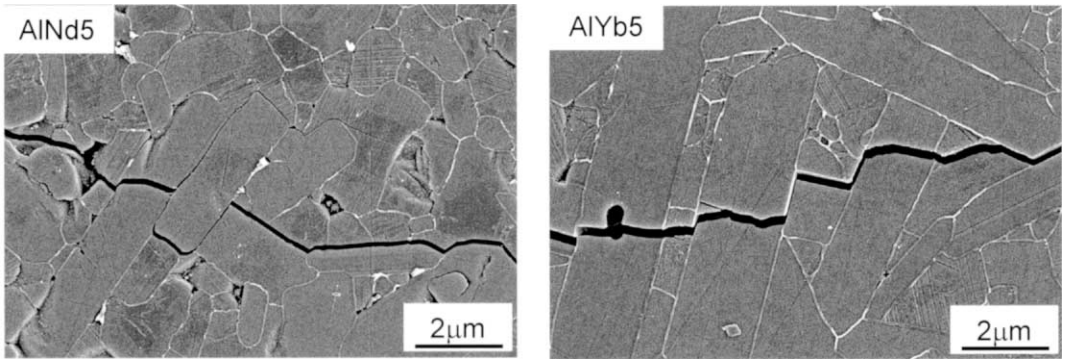

Fig. 8. SEM views of crack paths in the 1850 AlNd5 and the 1850 °C-annealed AlYb5 SiC materials.

α-SiC, and their true shape was plate-like as revealed by observations of the fracture surfaces. The present study has shown that the grain growth of SiC platelets was different for the SiC doped with different mixture additives of $RE_2O_3 + Al_2O_3$. As Hoffmann[28] reported that substitution of various rare-earth ions could significantly influence the growth rates of the rod-like β-Si_3N_4 grains, in this work the rare-earth ions should also have strong effects on the phase transformation and grain growth of SiC. Such effects deserve a continuing study in depth.

5. Conclusions

Four combinations of rare-earth oxides (RE_2O_3; RE = La, Nd, Y and Yb) and alumina were used as sintering additives for a fine β-SiC powder, and the mixed powders were hot-pressed and annealed. The microstructural development during annealing and the mechanical properties of the resulted materials were different for the SiC doped with different RE_2O_3 additives. That was attributed to the influences of the intergranular phase chemistry. For the specimens AlLa5 and AlNd5, into which the added RE_2O_3 were La_2O_3 and Nd_2O_3, respectively, high temperature annealing treatment could lead to simultaneous improvement of flexural strength and fracture toughness. The strength and toughness of the 1950 °C-annealed AlLa5 attained 661 MPa and 5.5 $MPa \cdot m^{1/2}$, respectively; and those for the 1950 °C-annealed AlNd5 were 620 MPa and 5.5 $MPa \cdot m^{1/2}$. It is suggested that the mechanical properties of liquid-phase-sintered SiC can improve to a new level by optimizing the intergranular phase chemistry and microstructure through judicious selection of sintering additives and annealing conditions.

Acknowledgements

This work has been supported by METI, Japan, as part of the Synergy Ceramics Project. The authors are members of the Joint Research Consortium of Synergy Ceramics.

References

1. Prochazka, S., The role of boron and carbon in the sintering of silicon carbide. In *Special Ceramics 6*, ed. P. Popper. British Ceramic Research Association, Stoke on Trent, 1975, pp. 171–181.
2. Padture, N. P., *In situ*-toughened silicon carbide. *J. Am. Ceram. Soc.*, 1994, **77**, 519–523.
3. Kim, Y.-W., Mitomo, M. and Hirotsuru, H., Grain growth and fracture toughness of fine-grained silicon carbide ceramics. *J. Am. Ceram. Soc.*, 1995, **78**, 3145–3148.
4. Cao, J. J., MoberlyChan, W. J., De Jonghe, L. C., Gilbert, C. J. and Ritchie, R. O., *In situ* toughened silicon carbide with Al–B–C additions. *J. Am. Ceram. Soc.*, 1996, **79**, 461–469.
5. Cho, D.-H., Kim, Y.-W. and Kim, W., Strength and fracture toughness of *in situ*-toughened silicon carbide. *J. Mater. Sci.*, 1997, **32**, 4777–4782.
6. Lee, C.-S., Kim, Y.-W., Cho, D.-H., Lee, H.-B. and Lim, H.-J., Microstructure and mechanical properties of self-reinforced alpha-silicon carbide. *Ceram. Int.*, 1998, **24**, 489–495.
7. Zhou, Y., Tanaka, H., Otani, S. and Bando, Y., Low-temperature pressureless sintering of α-silicon carbide with Al_4C_3–B_4C–C additives. *J. Am. Ceram. Soc.*, 1999, **82**, 1959–1964.
8. Zhan, G.-D., Mitomo, M. and Kim, Y.-W., Microstructural control for strengthening of silicon carbide ceramics. *J. Am. Ceram. Soc.*, 1999, **82**, 2924–2926.
9. Magnani, G., Minoccari, G. L. and Pilotti, L., Flexural strength and toughness of liquid phase sintered silicon carbide. *Ceram. Int.*, 2000, **26**, 495–500.
10. Sciti, D. and Bellosi, A., Influence of annealing treatments on microstructure and toughness of liquid-phase-sintered silicon carbide. *J. Mater. Res.*, 2001, **16**, 806–816.
11. Rixecker, G., Wiedmann, I., Rosinus, A. and Aldinger, F., High-temperature effects in the fracture mechanical behaviour of silicon carbide liquid-phase sintered with AlN-Y_2O_3 additives. *J. Eur. Ceram. Soc.*, 2001, **21**, 1013–1019.
12. Becher, P. F., Sun, E. Y., Hsueh, C.-H., Alexander, K. B., Hwang, S.-L., Waters, S. B. and Westmoreland, C. G., Debonding of interfaces between beta-silicon nitride whiskers and Si–Al–Y oxynitride glass. *Acta Mater.*, 1996, **44**, 3881–3893.
13. Sun, E. Y., Becher, P. F., Plucknett, K. P., Hsueh, C.-H., Alexander, K. B., Waters, S. B., Hirao, K. and Brito, M. E., Microstructure design of silicon nitride with improved fracture toughness: II, effects of yttria and alumina additives. *J. Am. Ceram. Soc.*, 1998, **81**, 2831–2840.

14. Kleebe, H.-J., Pezzotti, G. and Ziegler, G., Microstructure and fracture toughness of Si_3N_4 ceramics: combined roles of grain morphology and secondary phase chemistry. *J. Am. Ceram. Soc.*, 1999, **82**, 1857–1867.
15. Zhou, Y., Hirao, K., Toriyama, M., Yamauchi, Y. and Kanzaki, S., Effects of intergranular phase chemistry on the microstructure and mechanical properties of silicon carbide ceramics densified with rare-earth oxide and alumina additives. *J. Am. Ceram. Soc.*, 2001, **84**, 1642–1644.
16. Mizuno, M., Berjoan, R., Coutures, J. P. and Foex, M., System Al_2O_3–La_2O_3. In *Phase Diagrams for Ceramists,* (Vol. VI), ed. R. S. Roth, J. R. Dennis and H. F. McMurdie. 1987, The American Ceramic Society, Westerville, (Fig. 6438).
17. Mizuno, M., Yamada, T. and Noguchi, T., System Al_2O_3–Nd_2O_3. In *Phase Diagrams for Ceramists,* (Vol. VI), ed. R. S. Roth, J. R. Dennis and H. F. McMurdie. The American Ceramic Society, Westerville, 1987 (Fig. 6439).
18. Toropov, N. A., Bondar, I. A., Galakhov, F. Y., Nikogosyan, X. S. and Vinogradova, N. V., System Al_2O_3–Y_2O_3. In *Phase Diagrams for Ceramists,* (Vol. II), ed. E. M. Levin, C. R. Bobbins and H. F. McMurdie. The American Ceramic Society, Columbus, 1969 (Fig. 2344).
19. Bondar, I. A. and Toropov, N. A., System Al_2O_3–Yb_2O_3. In *Phase Diagrams for Ceramists, 1975 Supplement*, ed. E. M. Levin and H. F. McMurdie. The American Ceramic Society, Columbus, 1975 (Fig. 4371).
20. Chinn, R., Grain sizes of ceramics by automatic image analysis. *J. Am. Ceram. Soc.*, 1994, **77**, 589–592.
21. Kim, Y.-W., Mitomo, M. and Hirotsuru, H., Microstructural development of silicon carbide containing large seed grains. *J. Am. Ceram. Soc.*, 1997, **80**, 99–105.
22. Wotting, G., Kanka, B. and Ziegler, G., Microstructural development, microstructural characterization and relation to mechanical properties of dense silicon nitride. In *Non-oxide Technical and Engineering Ceramics*, ed. S. Hampshire. Elsevier Applied Science, London, 1986, pp. 83–96.
23. Sciti, D., Guicciardi, S. and Bellosi, A., Effect of annealing treatments on microstructure and mechanical properties of liquid-phase-sintered silicon carbide. *J. Eur. Ceram. Soc.*, 2001, **21**, 621–632.
24. Anstis, G. R., Chantikul, P., Lawn, B. R. and Marshall, D. R., A critical evaluation of indentation techniques for measuring fracture toughness: I, direct crack measurements. *J. Am. Ceram. Soc.*, 1981, **64**, 533–538.
25. Rice, R. W., Freiman, S. W. and Becher, P. F., Grain-size dependence of fracture energy in ceramics: I. Experimental. *J. Am. Ceram. Soc.*, 1981, **64**, 345–350.
26. Becher, P. F., Microstructural design of toughened ceramics. *J. Am. Ceram. Soc.*, 1991, **74**, 255–269.
27. Kim, Y.-W., Mitomo, M., Emoto, H. and Lee, J.-G., Effect of initial α-phase content on microstructure and mechanical properties of sintered silicon carbide. *J. Am. Ceram. Soc.*, 1998, **81**, 3136–3140.
28. Hoffmann, M. J., Analysis of microstructural development and mechanical properties of Si_3N_4 ceramics. In *Tailoring of Mechanical Properties of Si_3N_4 Ceramics*, ed. M. J. Hoffmann and G. Petzow. Kluwer Academic Publishers, Dordrecht, 1994, pp. 59–72.